Bayesian Feature Allocation Models for Natural Killer Cell Repertoire Studies Using Mass Cytometry Data

Arthur Lui

Advisor: Juhee Lee

Department of Applied Mathematics and Statistics
UC Santa Cruz

8 June 2018

Introduction

- **Cytometry at time-of-flight (CyTOF)**

  - commercialized in 2009

  - makes use of time-of-flight mass spectrometry to accelerate, separate, and identify ions by mass

  - enables detection of many parameters (biological, phenotypic, or functional markers) in less time and at a higher resolution [Cheung and Utz, 2011]

  - led to greater understanding of natural killer (NK) cells

Introduction

- **Natural Killer cells** play a critical role in cancer immunosurveillance

- NK cell diversity refers to number of NK cell sub-populations within NK cells, and also affects antiviral response

- Drs. Thall and Rezvani, collaborators at UT MD Anderson Cancer Center, have conducted clinical trials to study the potential clinical efficacy of umbilical cord blood (UCB) transplantation as a therapy for leukemia.

- In the trials, leukemia patients received UCB cell transplants, and NK cell surface protein markers are measured using mass cytometry.

- UCB NK cell therapy has the advantage of low risk of viral transmission from donor to recipient [Sarvaria et al., 2017].

CyTOF Data

	2B4	2DL1	2DL3	2DS4	3DL1	CCR7	$\cdots$
1	47.60	0.00	30.90	1.35	82.49	0.00	$\cdots$
2	81.84	0.44	0.88	0.51	176.99	2.38	$\cdots$
3	13.33	0.00	0.00	0.00	0.00	8.81	$\cdots$
4	23.64	3.37	43.39	0.27	0.73	0.00	$\cdots$
5	156.19	0.00	9.04	0.00	0.00	11.43	$\cdots$
6	273.86	0.00	9.71	2.41	0.84	0.52	$\cdots$
$\vdots$	$\vdots$	$\vdots$	$\vdots$	$\vdots$	$\vdots$	$\vdots$	$\vdots$
Cutoff	7.62	6.07	13.60	3.79	15.50	9.52	$\cdots$

Table 1: Cord-blood sample marker expression levels for 6 of 32 NK-cell markers (columns), and 6 of 41474 cells (rows). Last row contains cutoff values returned by CyTOF instrument.

- ▶ Data missing not at random
  - ▶ Some markers contain up to 85% missing values
- ▶ Cutoff values are computed after measurement

CyTOF Data

	2B4	2DL1	2DL3	2DS4	3DL1	CCR7	$\cdots$
1	1	0	1	0	1	0	$\cdots$
2	1	0	0	0	1	0	$\cdots$
3	1	0	0	0	0	0	$\cdots$
4	1	0	1	0	0	0	$\cdots$
5	1	0	0	0	0	1	$\cdots$
6	1	0	0	0	0	0	$\cdots$
$\vdots$	$\vdots$	$\vdots$	$\vdots$	$\vdots$	$\vdots$	$\vdots$	
Cutoff	7.62	6.07	13.60	3.79	15.50	9.52	$\cdots$

Table 2: Cell phenotypes (rows)

▶ Obtaining cell phenotypes using overly-simplistic methods may yield unreasonably high number of sub-populations.

Existing Methods

- Most existing methods use traditional clustering methods (K-means, hierarchical clustering, density-based clustering, nearest-neighbor clustering, etc.)

- For high-dimensional cytometry data, Weber and Robinson [2016] compared existing clustering methods including **FlowSOM** [Van Gassen et al., 2015], **PhenoGraph** [Levine et al., 2015], **Rclusterpp** [Linderman et al., 2013], and **flowClust** [Lo et al., 2009]

- Existing methods do not directly model latent phenotypes or quantify model uncertainty

Proposed Projects

- **Project I**: Bayesian Feature Allocation Model for Heterogeneous Cell Populations

- **Project II**: Repulsive Feature Allocation Model

- **Project III**: Feature Allocation Model with Regression for Abundances of Features in Longitudinal Data

Project I

Feature Allocation Model – Indian buffet process

Griffiths and Ghahramani [2011] introduced the IBP as follows:

Let $\mathbf{Z}$ be a $J \times K$ matrix such that

$$
\begin{aligned}
z_{jk} \mid \pi_k &\sim \text{Bernoulli}(\pi_k) \\
\pi_k \mid \alpha &\sim \text{Beta}(\alpha/K, 1)
\end{aligned}
$$

for $j = 1, \cdots J$ and $k = 1, \cdots, K$, and where α is positive.

Feature Allocation Model – Indian buffet process

Griffiths and Ghahramani [2011] introduced the IBP as follows:

Let $\boldsymbol{Z}$ be a $J \times K$ matrix such that

$$
\begin{aligned}
z_{jk} \mid \pi_k &\sim \text{Bernoulli}(\pi_k) \\
\pi_k \mid \alpha &\sim \text{Beta}(\alpha/K, 1)
\end{aligned}
$$

for $j = 1, \cdots J$ and $k = 1, \cdots, K$, and where α is positive.
Then as $K \to \infty$, $\boldsymbol{Z} \sim \text{IBP}(\alpha)$.

Feature Allocation Model – Indian buffet process

Griffiths and Ghahramani [2011] introduced the IBP as follows:

Let $\boldsymbol{Z}$ be a $J \times K$ matrix such that

$$\begin{aligned}
z_{jk} \mid \pi_k &\sim \text{Bernoulli}(\pi_k) \\
\pi_k \mid \alpha &\sim \text{Beta}(\alpha/K, 1)
\end{aligned}$$

for $j = 1, \cdots J$ and $k = 1, \cdots, K$, and where α is positive.
Then as $K \to \infty$, $\boldsymbol{Z} \sim \text{IBP}(\alpha)$. It can be shown that

$$P(\boldsymbol{Z}) = \frac{\alpha^{K_+}}{\prod_{h=1}^{2^J-1} K_h!} \exp\{-\alpha H_J\} \prod_{k=1}^{K_+} \frac{(J-m_k)!(m_k-1)!}{J!},$$

where $H_J = \sum_{j=1}^{J} j^{-1}$ is the harmonic number, K_+ is the number of non-zero columns in $\boldsymbol{Z}$, m_k is the kth column sum of $\boldsymbol{Z}$, and K_h the number of columns having history h (some binary number).

Z ~ IBP(5)
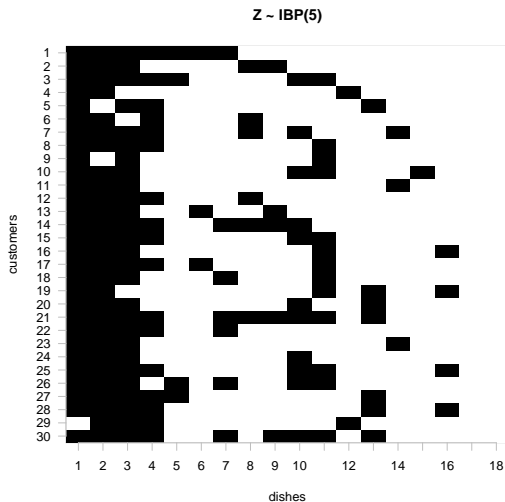
Project I: Bayesian Feature Allocation Model for Heterogeneous Cell Populations

Notation

- I: Number of samples
- J: Number of markers
- N_i: Number of observations in sample i
- $\tilde{y}_{inj}$: Raw expression levels for observation n in sample i for marker j. ($\tilde{y}_{inj} \geq 0$)
- c_{ij}: Cutoff for marker j, sample i
- y_{inj}: Transformed expression levels for observation n, sample i, marker j

$$y_{inj} = \log\left(\frac{\tilde{y}_{inj}}{c_{ij}}\right) \in \mathbb{R}.$$

  - ($y_{inj} \gg 0$) likely corresponds to expression
  - ($y_{inj} \ll 0$) likely corresponds to non-expression

Project I: Bayesian Feature Allocation Model for Heterogeneous Cell Populations

- **Z**: $(J \times K)$ binary matrix defining the latent phenotypes.
    - if $Z_{jk} = 1$, then marker j is expressed in phenotype k
    - if $Z_{jk} = 0$, then marker j is not expressed in phenotype k
- K is a sufficiently large constant
- $\lambda_{in} \in \{1, ..., K\}$: The latent phenotype of observation n, sample i

Project I: Sampling Distribution

$$y_{inj} \mid \eta_{ij}, \boldsymbol{\mu}^\star, \sigma_i^{2\star} \overset{ind}{\sim} \begin{cases} F_0, & \text{if } z_{j,\lambda_{in}} = 0, \\ F_1, & \text{if } z_{j,\lambda_{in}} = 1. \end{cases}$$

$$y_{inj} \mid \boldsymbol{\eta}_{ij}, \boldsymbol{\mu}^\star, \boldsymbol{\sigma}_i^{2\star} \stackrel{ind}{\sim} \begin{cases} F_0, & \text{if } z_{j,\lambda_{in}} = 0, \\ F_1, & \text{if } z_{j,\lambda_{in}} = 1. \end{cases}$$

- $F_0 = \sum_{\ell=1}^{L^0} \eta_{ij\ell}^0 \text{ Normal}(\mu_{0\ell}^\star, \sigma_{0i\ell}^{2\star})$, where $\mu_{0\ell}^\star < 0$
- $F_1 = \sum_{\ell=1}^{L^1} \eta_{ij\ell}^1 \text{ Normal}(\mu_{1\ell}^\star, \sigma_{1i\ell}^{2\star})$, where $\mu_{1\ell}^\star > 0$
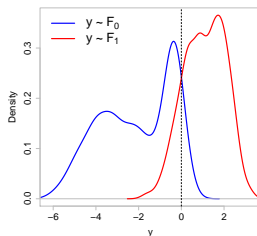
Figure 1: Kernel density estimate of samples from F_0 (blue) and F_1 (red)

$$m_{inj} \mid p_{inj} \stackrel{ind}{\sim} \text{Bernoulli}(p_{inj})$$

Project I: Missing Mechanism

$$m_{inj} \mid p_{inj} \overset{ind}{\sim} \text{Bernoulli}(p_{inj})$$

$$\text{logit}(p_{inj}) = \begin{cases} \beta_{0i} - \beta_{1i}(y_{inj} - c_0)^2, & \text{if } y_{inj} < c_0 \\ \beta_{0i} - \beta_{1i}c_1\,(y_{inj} - c_0)^{1/2}, & \text{otherwise,} \end{cases}$$

where $m_{inj} = 1$ if y_{inj} is missing, and 0 otherwise.
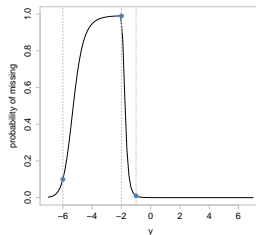
Figure 2: Example missing mechanism

Project I: Priors

Latent Phenotypes

$$
\begin{aligned}
\boldsymbol{Z} \mid \alpha &\sim \text{IBP}_K(\alpha) \\
\alpha &\sim \text{Gamma}(a_\alpha, b_\alpha)
\end{aligned}
$$

Project I: Priors

Latent Phenotypes

$$z_{jk} \mid v_k \overset{ind}{\sim} \text{Bernoulli}(v_k)$$
$$v_k \mid \alpha \overset{iid}{\sim} \text{Beta}(\alpha/K, 1)$$
$$\alpha \sim \text{Gamma}(a_\alpha, b_\alpha)$$

Project I: Priors

Latent Phenotypes

$$
\begin{aligned}
z_{jk} \mid h_{jk}, v_k &= \mathbb{I}\left\{\Phi(h_{jk} \mid 0, 1) < v_k\right\} \\
v_k \mid \alpha &\overset{iid}{\sim} \text{Beta}(\alpha/K, 1) \\
\boldsymbol{h}_k &\overset{iid}{\sim} \text{Normal}_J(\mathbf{0}, \mathbf{I}) \\
\alpha &\sim \text{Gamma}(a_\alpha, b_\alpha)
\end{aligned}
$$

Project I: Priors

Latent Phenotypes

$$
\begin{aligned}
z_{jk} \mid h_{jk}, v_k &= \mathbb{I}\left\{ \Phi(h_{jk} \mid 0, \Gamma_{jj}) < v_k \right\} \\
v_k \mid \alpha &\overset{iid}{\sim} \text{Beta}(\alpha/K, 1) \\
\boldsymbol{h}_k &\overset{iid}{\sim} \text{Normal}_J(\boldsymbol{0}, \Gamma) \\
\alpha &\sim \text{Gamma}(a_\alpha, b_\alpha)
\end{aligned}
$$

▶ Dependent IBP (dIBP) [Williamson et al., 2010] construction to model correlations between markers

▶ dIBP reduces to IBP [Griffiths and Ghahramani, 2011] when Γ is the identity matrix

Project I: Priors

Latent Phenotypes

$$\mathbf{Z} \mid \alpha, \Gamma \quad \sim \quad \mathrm{dIBP}_K(\alpha, \Gamma)$$
$$\alpha \quad \sim \quad \mathrm{Gamma}(a_\alpha, b_\alpha)$$

▶ Dependent IBP (dIBP) [Williamson et al., 2010] construction to model correlations between markers
▶ dIBP reduces to IBP [Griffiths and Ghahramani, 2011] when Γ is the identity matrix

Project I: Priors

Phenotype Abundance

Let w_{ik} denote an abundance level of phenotype k in sample i. Let $\boldsymbol{w}_i = (w_{i1}, \ldots, w_{iK})$. Then, $\boldsymbol{w}_i \mid K \overset{iid}{\sim} \text{Dirichlet}_K(d/K)$.

Latent Cell Phenotype Indicators

$$p(\lambda_{in} = k \mid \boldsymbol{w}_i) = w_{ik}$$

Project I: Priors

$$\mu_{0\ell}^{\star} \mid \psi_0, \tau_0^2 \overset{iid}{\sim} \text{Normal}_-(\psi_0, \tau_0^2), \quad \ell \in \left\{1, ..., L^0\right\}$$

$$\mu_{1\ell}^{\star} \mid \psi_1, \tau_1^2 \overset{iid}{\sim} \text{Normal}_+(\psi_1, \tau_1^2), \quad \ell \in \left\{1, ..., L^1\right\}$$

$$\sigma_{0i\ell}^2 \mid s_i \overset{ind}{\sim} \text{Inverse-Gamma}(a_\sigma, s_i), \quad \ell \in \left\{1, ..., L^0\right\}$$

$$\sigma_{1i\ell}^2 \mid s_i \overset{ind}{\sim} \text{Inverse-Gamma}(a_\sigma, s_i), \quad \ell \in \left\{1, ..., L^1\right\}$$

$$s_i \overset{iid}{\sim} \text{Gamma}(a_s, b_s), \quad i \in \{1, ..., I\}$$

$$\eta_{ij}^0 \overset{iid}{\sim} \text{Dirichlet}_{L^0}(a_{\eta^0}/L^0), \quad i \in \{1, ..., I\}, j \in \{1, ..., J\}$$

$$\eta_{ij}^1 \overset{iid}{\sim} \text{Dirichlet}_{L^1}(a_{\eta^1}/L^1), \quad i \in \{1, ..., I\}, j \in \{1, ..., J\}$$

$$\beta_{0i} \overset{iid}{\sim} \text{Normal}(m_{\beta_0}, s_{\beta_0}^2), \quad i \in \{1, ..., I\}$$

$$\beta_{1i} \overset{iid}{\sim} \text{Normal}_+(m_{\beta_1}, s_{\beta_1}^2), \quad i \in \{1, ..., I\}$$

Project I: Posterior Estimate for Z

- Z susceptible to label switching, especially when K is random

- We summarize the posterior distribution of Z using sequentially-allocated latent structure optimization (SALSO) [Dahl and Müller, 2017]

Project I: Posterior Estimate for **Z**

For each posterior sample $b \in \{1, ..., B\}$ and patient sample i,

1. compute a $(J \times J)$ Adjacency Matrix $A_i^{(b)}$, where

$$A_{i_{j,j'}}^{(b)} = \sum_{k=1}^{K} w_{ik}^{(b)} \mathbb{1}\left\{z_{jk}^{(b)} = z_{j'k}^{(b)} = 1\right\}$$

2. compute the mean adjacency matrix $\bar{A}_i = \sum_{b=1}^{B} A_i^{(b)}/B$.

3. $\hat{\boldsymbol{Z}}_i = \text{argmin}_{\boldsymbol{Z}} \sum_{j,j'} (A_{i_{j,j'}}^{(b)} - \bar{A}_{i_{j,j'}})^2$

Figure 3: Simulation truth for Z in Sample 1, with markers in rows and latent phenotypes in columns. Black and white represents $z_{jk} = 1$ and 0, respectively. The phenotypes and w_1 are shown at the bottom and on top, respectively. The markers are sorted by w_{ik}.

Figure 4: Simulated data for one sample
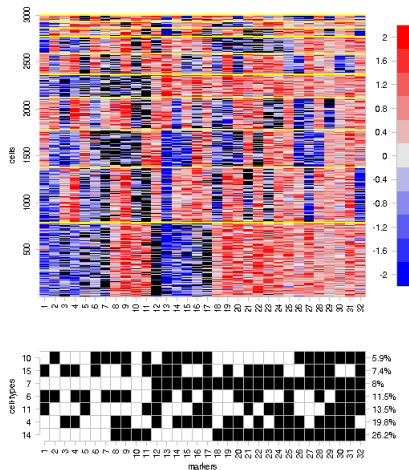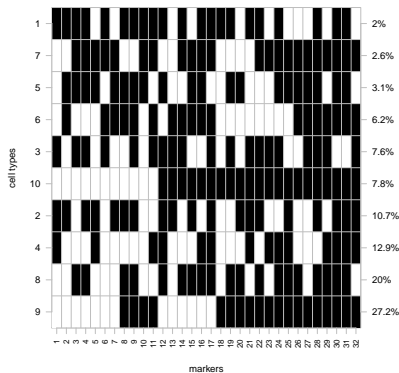
(a) Sample 1 (b) Z true

Figure 5: FAM Simulation Study
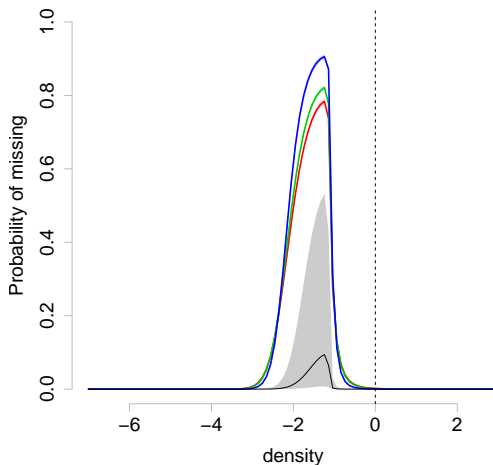
Figure 6: Posterior missing mechanism for simulation study in Project I for sample 1 (red), 2 (green), and 3 (blue). Prior missing mechanism in grey.

(a) Sample 1   (b) Z true

Figure 7: FlowSOM Simulation Study

Project I: Simulation Study – Comparing FAM and FlowSOM

We use the F-score to summarize the accuracy of the computed cluster labels. The F-score is defined as the harmonic mean of precision and recall.

$$F_1 = \frac{2}{\text{precision}^{-1} + \text{recall}^{-1}},$$

- precision $=$ (true positives) $/$ (true positives $+$ false positives)
- recall $=$ (true positives) $/$ (true positives $+$ false negatives)
- $F_1 \in [0, 1]$ with $F_1 = 1$ being a perfect score

	F-score	Elapsed time (seconds)
FlowSOM	0.490	6
FAM	0.999	17472

Table 3: F-score and elapsed time for simulated data for FAM and FlowSOM

Project I: Conclusions for Comparing FAM and FlowSOM

- ▶ FAM produces posterior distribution and estimates of latent phenotypes and their weights

- ▶ Choose K sufficiently large

- ▶ Graph first two principal components to visually estimate K

- ▶ FlowSOM quickly produces point estimates of clusters

- ▶ In FlowSOM, additional ad-hoc criteria are needed to produce estimates of latent phenotypes and their abundance

- ▶ In FlowSOM, missing values need to be pre-imputed

Project I: Cord Blood Samples Data

- Three cord blood (CB) samples from MD Anderson Cancer Center

- Number of cells in each sample $N = (41474, 10454, 5177)$

- Number of markers $J = 32$

- $K = 20$

- MCMC: 2000 iterations, 1000 burn-in
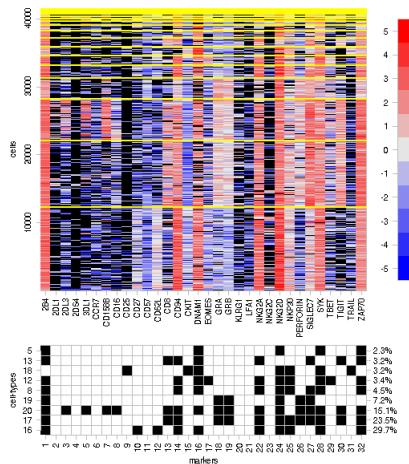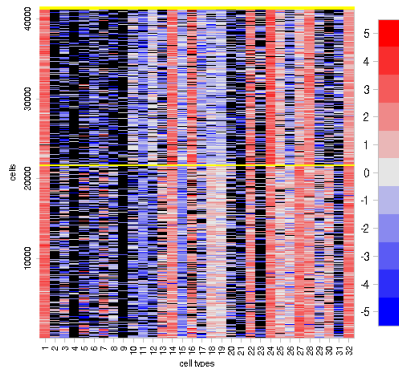
Sample 1 (FAM)   Sample 1 (FlowSOM)

Figure 8: CB data Sample 1, analyzed using FAM (left) and FlowSOM (right)
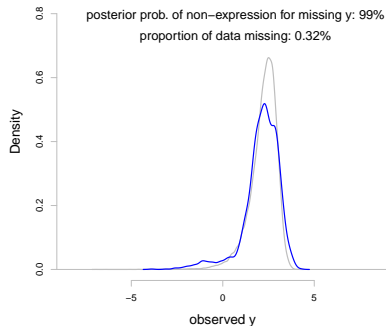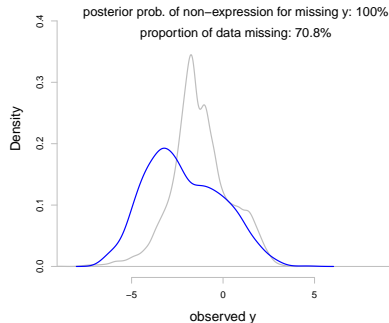
(a) Sample 1, marker 1   (b) Sample 1, marker 2

Figure 9: Observed data density for y_{ij} in grey. Posterior predictive density for observed data in blue.
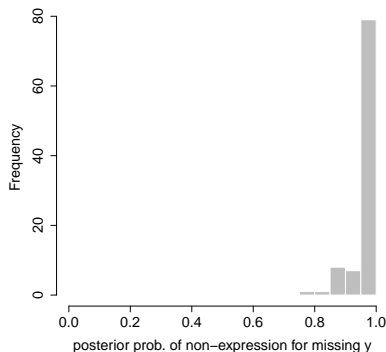
Figure 10: Histogram of posterior probabilities $\hat{q}_{ij}$ of non-expression for missing for all (i, j). The peak at 1 suggests a marker is not likely expressed if its expression level is missing.

R Package

```R
# R code for installing cytof3

library(devtools)
repo = 'luiarthur/ucsc_litreview'
subdir = 'cytof/src/model3/cytof3'
install_github(repo, subdir=subdir)
```

Project II

Project II: Repulsive Feature Allocation Model

- ▶ Similar or duplicated features may occur in feature allocation matrix under IBP prior

- ▶ Repulsion penalizes similar features in the prior, resulting in a parsimonious model

- ▶ Different approaches for repulsive models have been developed mostly in the context of mixture models [Petralia et al., 2012, Quinlan et al., 2017b, Xie and Xu, 2017, Quinlan et al., 2017a].

Project II: Repulsive Feature Allocation Model

Objective

- Develop a repulsive feature allocation model for parsimonious feature matrix

- Compare phenotypes present in healthy subject samples and cord blood samples

- Sample covariate x_i. Cord blood samples ($x_i = 0$). Healthy subject samples ($x_i = 1$).
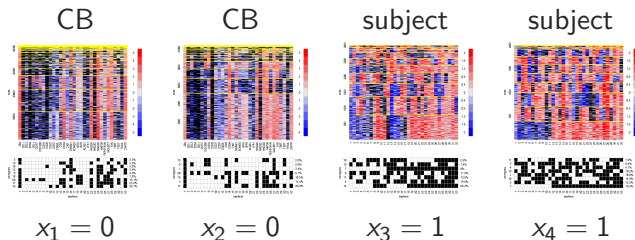
CB	CB	subject	subject
$x_1 = 0$	$x_2 = 0$	$x_3 = 1$	$x_4 = 1$

- Sample covariate x_i. Cord blood samples ($x_i = 0$). Healthy subject samples ($x_i = 1$).

CB	CB	subject	subject
$x_1 = 0$	$x_2 = 0$	$x_3 = 1$	$x_4 = 1$
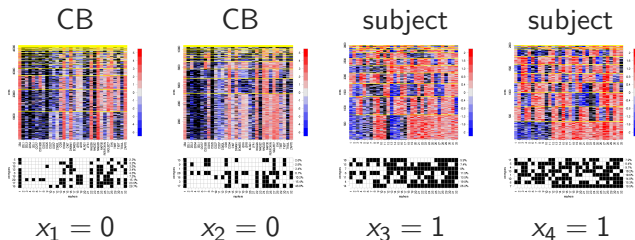
- Learn binary indicator $\delta_{xk} \in \{0, 1\}$, $x = 0, 1$, and $k = 1, \ldots, K$, to indicate whether samples from x possess phenotype k

$$P(\mathbf{Z} \mid v) \propto \prod_{k=1}^{K} \left\{ \prod_{j=1}^{J} v_k^{z_{jk}} (1 - v_k)^{1-z_{jk}} \right\}$$

$$v_K \mid \alpha \sim \text{Beta}(\alpha/K, 1)$$

Project II: rep-FAM Prior

$$P(\mathbf{Z} \mid v, C_\phi) \propto \prod_{k=1}^{K} \left\{ \prod_{j=1}^{J} v_k^{z_{jk}}(1 - v_k)^{1-z_{jk}} \right\} \times$$

$$\prod_{k_1=1}^{K-1} \prod_{k_2=k_1+1}^{K} \left\{ 1 - C_\phi \left(\rho(\mathbf{z}_{k_1}, \mathbf{z}_{k_2}) \right) \right\}$$

$$v_K \mid \alpha \sim \text{Beta}(\alpha/K, 1)$$

where

- $C_\phi(\cdot)$ is a continuous decreasing function in distance with $C_\phi(0) = 1$ and $\lim_{d \to \infty} C_\phi(d) = 0$.

- $\rho(\mathbf{z}_{k_1}, \mathbf{z}_{k_2})$ is a distance metric

- We use $C_\phi(d) = C(d) = \exp\{-d\}$, and $\rho(\mathbf{z}_{k_1}, \mathbf{z}_{k_2}) = \sum_{j=1}^{J} |z_{jk_1} - z_{jk_2}|$
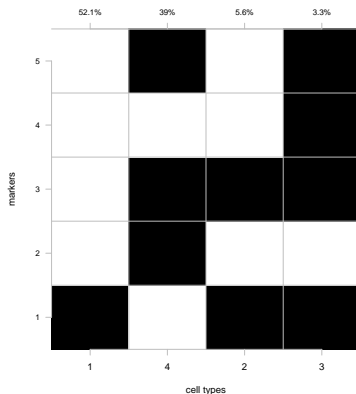
Figure 11: Simulation truth for Z in Sample 1, with markers in rows and latent phenotypes in columns. Black and white represents $z_{jk} = 1$ and 0, respectively. The phenotypes and w_1 are shown at the bottom and on top, respectively. The markers are sorted by w_{ik}.
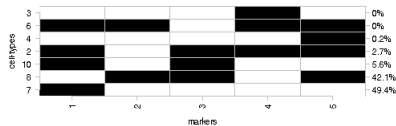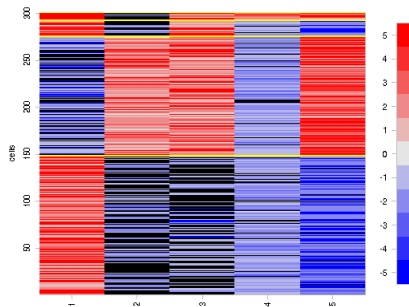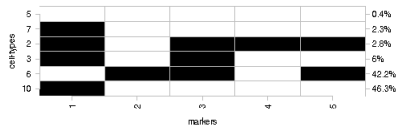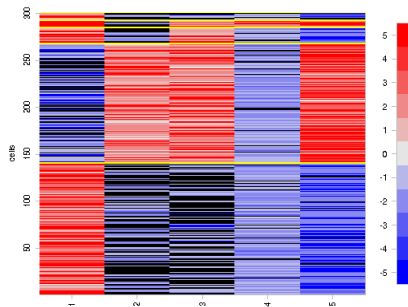
(a) rep-FAM   (b) IBP

Figure 12: Heatmaps of y for simulated data ordered by phenotypes (Sample 1)

Project III

Project III: Feature Allocation Model with Regression for Feature Abundances Over Time

Objectives:

1. Extend the previous models to analyze samples taken at multiple time points from a patient after NK cell infusion.

2. Model the evolution of NK cell populations over time

Project III: Feature Allocation Model with Regression for Feature Abundances Over Time

- I samples taken at time points $t_1, ..., t_I$

- Phenotype abundances $\boldsymbol{w}_{t_i} = (w_{t_i,1}, \ldots, w_{t_i,K})$ as a function of time (t_i) after treatment

- $\boldsymbol{Z}$ includes possible cell types possessed across all samples

Project	Academic Quarter
Project 1	Fall 17 - Fall 18
Project 2	Fall 18 - Spring 19
Project 3	Winter 19 - Fall 19
Thesis	Fall 19 - Winter 20

I

Appendix

Regina K Cheung and Paul J Utz. Screening: Cytof - the next generation of cell detection. *Nature Reviews Rheumatology*, 7(9): 502, 2011.

David B. Dahl and Peter Müller. Summarizing distributions of latent structures. *Bayesian Nonparametric Inference: Dependence Structures & Applications Oaxaca, Mexico*, 2017.

Thomas L Griffiths and Zoubin Ghahramani. The indian buffet process: An introduction and review. *Journal of Machine Learning Research*, 12(Apr):1185–1224, 2011.

Jacob H Levine, Erin F Simonds, Sean C Bendall, Kara L Davis, D Amir El-ad, Michelle D Tadmor, Oren Litvin, Harris G Fienberg, Astraea Jager, Eli R Zunder, et al. Data-driven phenotypic dissection of aml reveals progenitor-like cells that correlate with prognosis. *Cell*, 162(1):184–197, 2015.

Michael Linderman, Robert Bruggner, and Maintainer Robert Bruggner. Package 'rclusterpp'. 2013.

Kenneth Lo, Florian Hahne, Ryan R Brinkman, and Raphael Gottardo. flowclust: a bioconductor package for automated gating of flow cytometry data. *BMC bioinformatics*, 10(1):145, 2009.

Francesca Petralia, Vinayak Rao, and David B Dunson. Repulsive mixtures. In *Advances in Neural Information Processing Systems*, pages 1889–1897, 2012.

José Quinlan, Fernando A Quintana, and Garritt L Page. Density regression using repulsive distributions. 2017a.

José J Quinlan, Fernando A Quintana, and Garritt L Page. Parsimonious hierarchical modeling using repulsive distributions. *arXiv preprint arXiv:1701.04457*, 2017b.

Anushruti Sarvaria, Dunia Jawdat, J Alejandro Madrigal, and Aurore Saudemont. Umbilical cord blood natural killer cells, their characteristics, and potential clinical applications. *Frontiers in Immunology*, 8, 2017.

Sofie Van Gassen, Britt Callebaut, Mary J Van Helden, Bart N Lambrecht, Piet Demeester, Tom Dhaene, and Yvan Saeys. Flowsom: Using self-organizing maps for visualization and interpretation of cytometry data. *Cytometry Part A*, 87(7): 636–645, 2015.

Lukas M Weber and Mark D Robinson. Comparison of clustering methods for high-dimensional single-cell flow and mass cytometry data. *Cytometry Part A*, 89(12):1084–1096, 2016.

Sinead Williamson, Peter Orbanz, and Zoubin Ghahramani. Dependent indian buffet processes. In *International Conference on Artificial Intelligence and Statistics*, pages 924–931, 2010.

Fangzheng Xie and Yanxun Xu. Bayesian repulsive gaussian mixture model. *arXiv preprint arXiv:1703.09061*, 2017.

Missing Mechanism Posterior
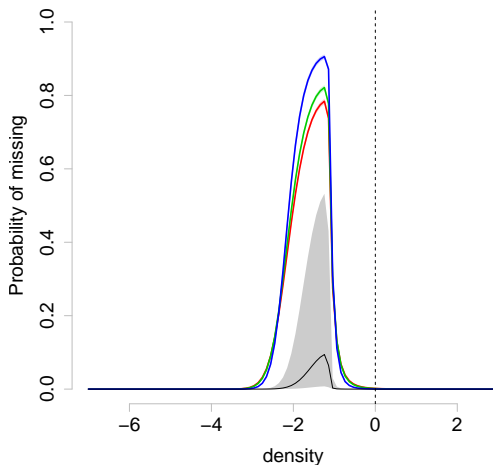
Figure 13: Posterior missing mechanism for simulation study in Project I for sample 1 (red), 2 (green), and 3 (blue). Prior missing mechanism in grey.
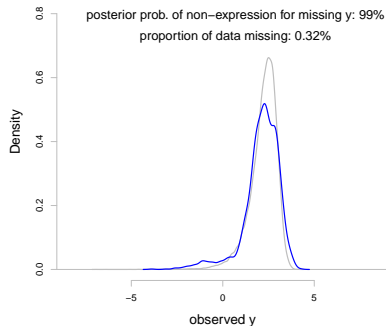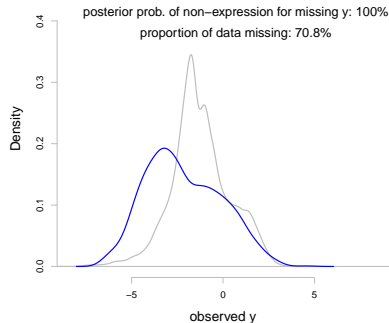
(a) Sample 1, marker 1　　　(b) Sample 1, marker 2

Figure 14: Observed data density for y_{ij} in grey. Posterior predictive density for observed data in blue.
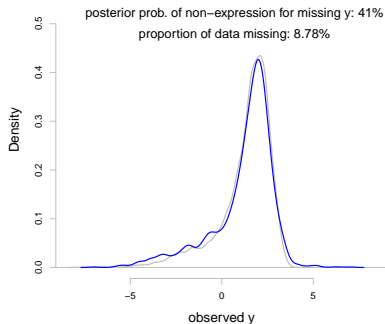
(c) Sample 2, marker 22
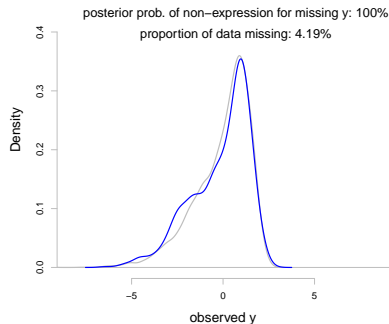
(d) Sample 3, marker 19

Figure 15: Observed data density for y_{ij} in grey. Posterior predictive density for observed data in blue.

Probability of Non-expression for Imputed Values in Project I CB Analysis
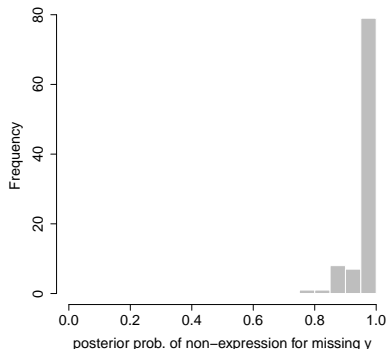
Figure 16: Histogram of posterior probabilities $\hat{q}_{ij}$ of non-expression for missing for all (i, j). The peak at the value of 1 suggests that most of the time, a marker is estimated as no expression if its expression level is missing.
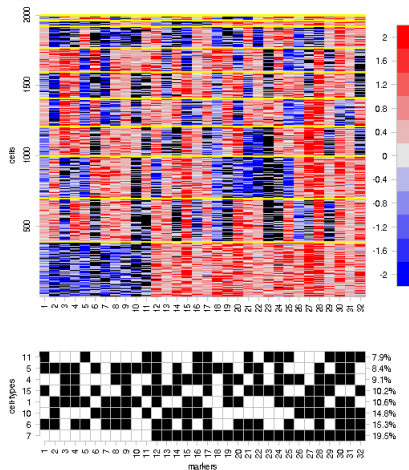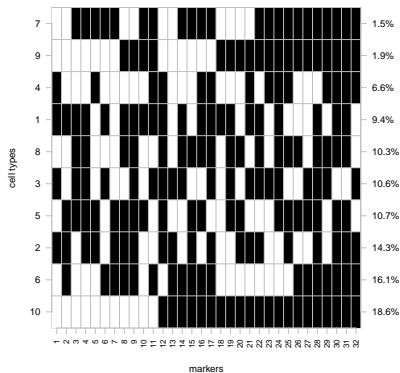
(a) Sample 2

(b) Z true

Figure 17: FAM Simulation Study
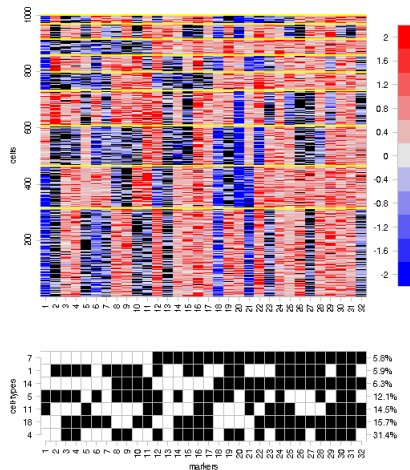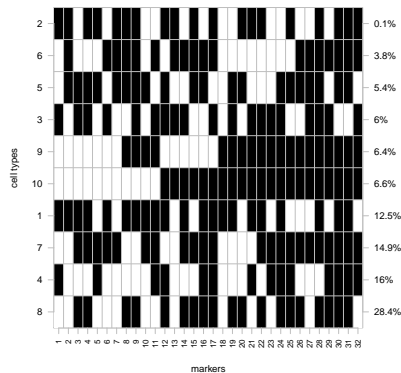
(a) Sample 3

(b) Z true

Figure 18: FAM Simulation Study
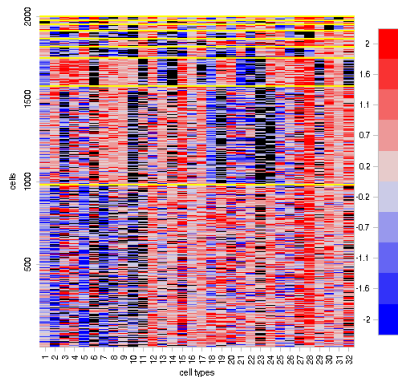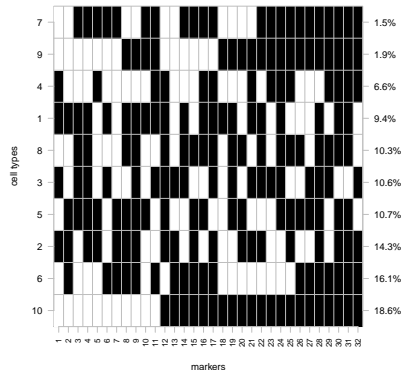
(a) Sample 2   (b) Z true

Figure 19: FlowSOM Simulation Study
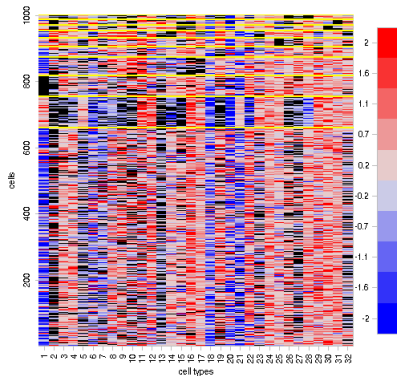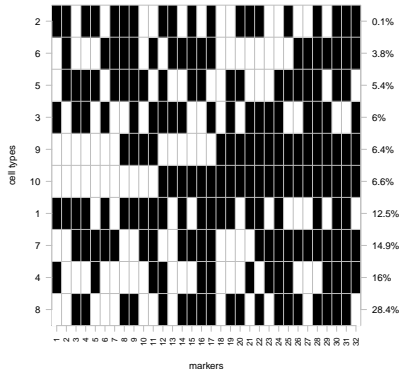
(a) Sample 3   (b) Z true

Figure 20: FlowSOM Simulation Study
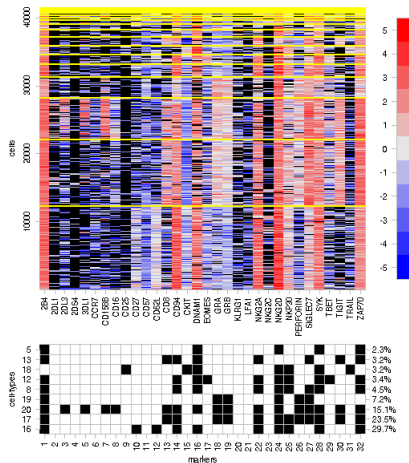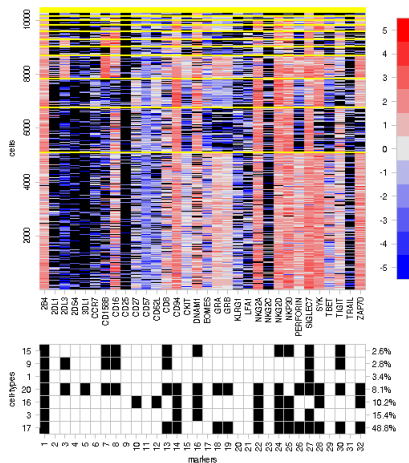
(a) Sample 1   (b) Sample 2

Figure 21: CB data analyzed using FAM
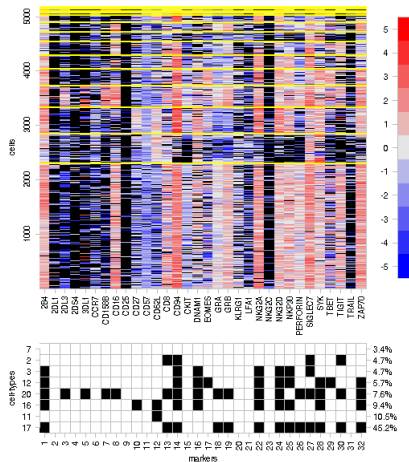
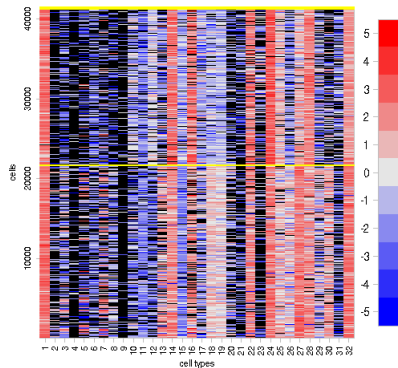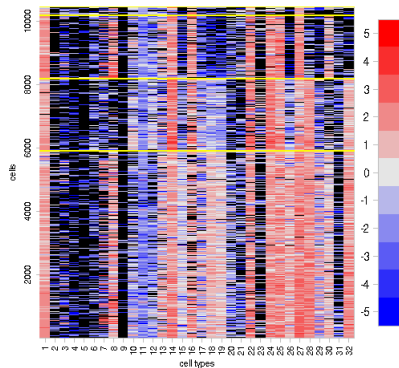(c) Sample 3

Figure 22: CB data analyzed using FAM
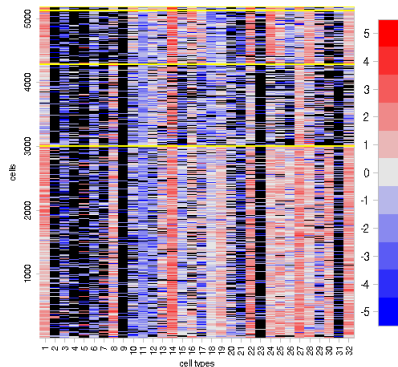
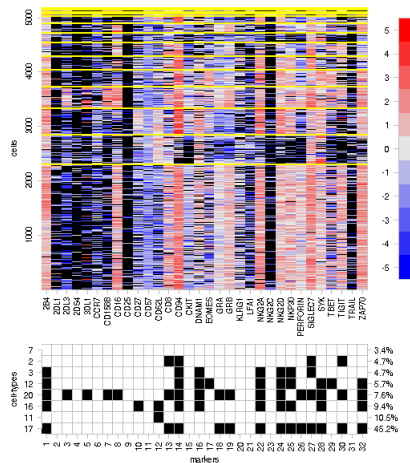(a) Sample 1   (b) Sample 2

Figure 23: CB data analyzed using FlowSOM

Sample 3 (FlowSOM)   Sample 3 (FAM)

Figure 24: CB data Sample 3, analyzed using FlowSOM (left) and FAM (right)
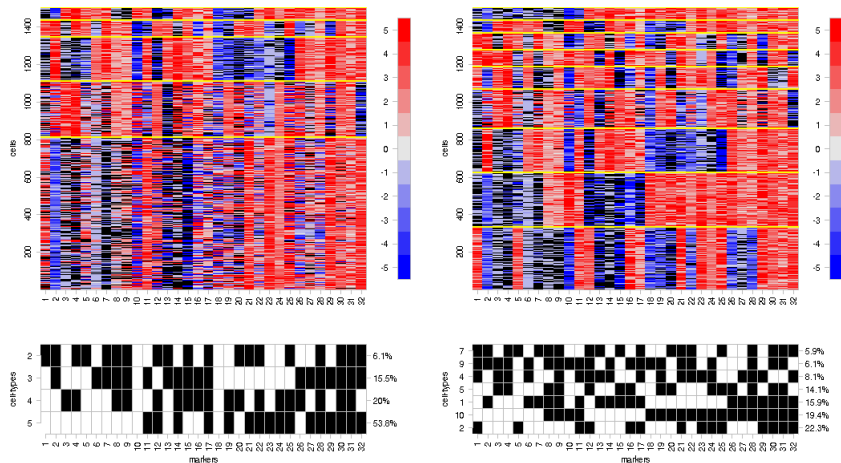
(a) Sample 1. $K = 5$

(b) Sample 1. $K = 10$

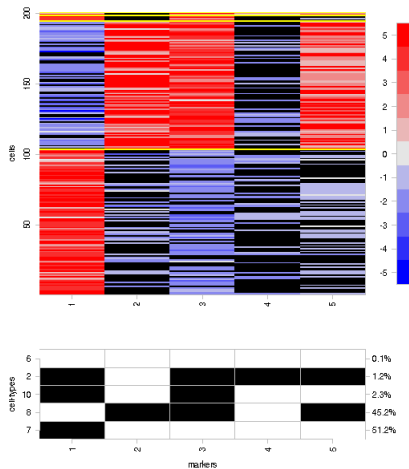Figure 25: FAM sensitivity to K

(c) Sample 1. $K = 20$ (b) Sample 1. $K = 10$

Figure 26: FAM sensitivity to K

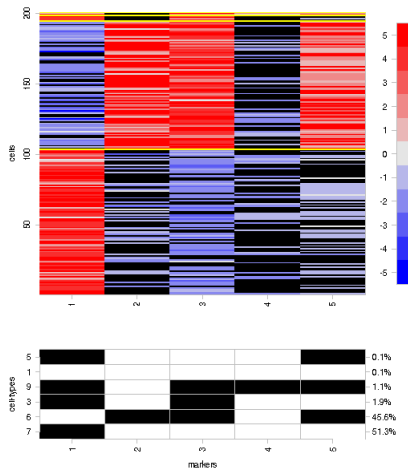# Project I: Conclusions for FAM's Sensitivity to K

- Choose K sufficiently large

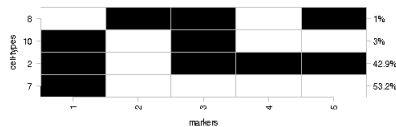- May graph first two principal components to visually estimate K

(a) rep-FAM (b) IBP

Figure 27: Heatmaps of y for simulated data ordered by phenotypes (Sample 2)

(a) rep-FAM   (b) IBP

Figure 28: Heatmaps of y for simulated data ordered by phenotypes (Sample 3)

Z ~ IBP(5)

Why is it called the Indian Buffet Process?

In the IBP, a customer (j) taking a dish (k) is analogous to an observation possessing a feature. This is indicated by setting the value of z_{jk} to 1 if the customer takes the dish, and 0 otherwise. An IBP(α) for J observations can be simulate as follows:

1. The 1st customer takes Poisson(α) number of dishes
2. For customers $j = 2$ to J,
   - For each previously sampled dish, customer j takes dish k with probability m_k/j
   - after sampling the last sampled dish, customer j samples Poisson(α/j) new dishes

It can be shown that a matrix generated by this process has the same pmf up to a proportionality constant as the previous pmf.

One draw from the IBP

Z ~ IBP(5)

Z ~ IBP(5)
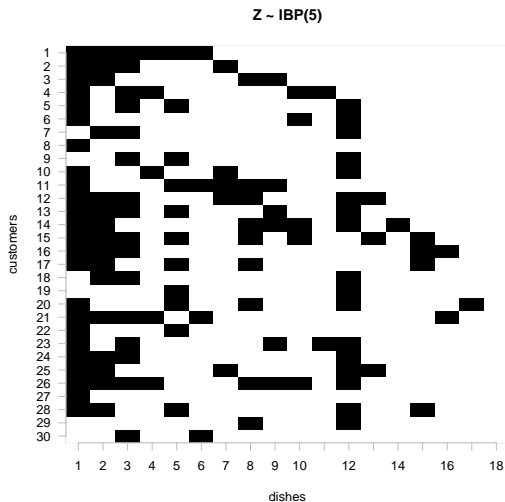
Expected value of the IBP

E[Z] ~ IBP(5)
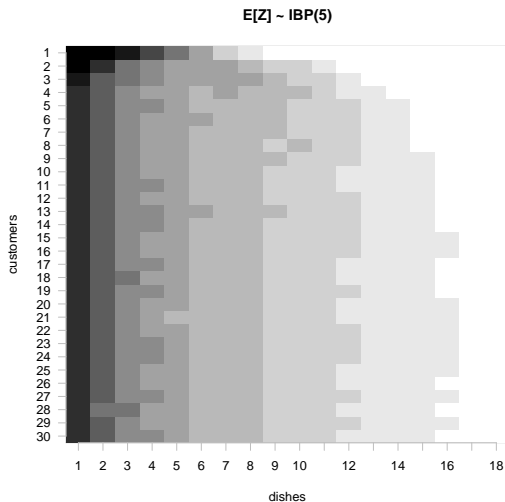
Project II: Simulation Study for rep-FAM Prior
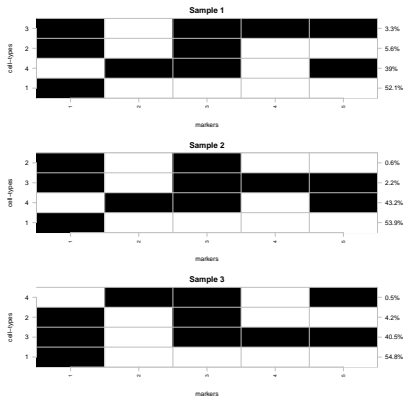
Figure 29: The transpose of $\boldsymbol{Z}^{\text{TR}}$ with markers in columns and latent phenotypes in rows. Black and white represents $z_{jk}^{\text{TR}} = 1$ and 0, respectively. The phenotypes and $\boldsymbol{w}_i^{\text{TR}}$ are shown on the left and right sides of each panel. All samples share the same $\boldsymbol{Z}^{\text{TR}}$ and the phenotypes are arranged in order of w_{ik}^{TR} within each sample.

Project II: Feature Selection for Different Samples

- Sample covariate x_i. Cord blood samples ($x_i = 0$). Healthy subject samples ($x_i = 1$).

Project II: Feature Selection for Different Samples

- ► Sample covariate x_i. Cord blood samples ($x_i = 0$). Healthy subject samples ($x_i = 1$).
- ► Binary indicator $\delta_{xk} \in \{0, 1\}$, $x = 0, 1$, and $k = 1, \ldots, K$, to indicate whether samples from x possess phenotype k

Project II: Feature Selection for Different Samples

- Sample covariate x_i. Cord blood samples ($x_i = 0$). Healthy subject samples ($x_i = 1$).
- Binary indicator $\delta_{xk} \in \{0, 1\}$, $x = 0, 1$, and $k = 1, \ldots, K$, to indicate whether samples from x possess phenotype k
- $\delta_{xk} \mid p_x \overset{ind}{\sim}$ Bernoulli(p_x) and $p_x \overset{iid}{\sim}$ Beta(a_p, b_p).

Project II: Feature Selection for Different Samples

- ▶ Sample covariate x_i. Cord blood samples ($x_i = 0$). Healthy subject samples ($x_i = 1$).
- ▶ Binary indicator $\delta_{xk} \in \{0, 1\}$, $x = 0, 1$, and $k = 1, \ldots, K$, to indicate whether samples from x possess phenotype k
- ▶ $\delta_{xk} \mid p_x \overset{ind}{\sim}$ Bernoulli(p_x) and $p_x \overset{iid}{\sim}$ Beta(a_p, b_p).
- ▶ Unnormalized cell phenotype abundances
  $\tilde{w}_{ik} \overset{ind}{\sim}$ Gamma($a_W/K, 1$), $i = 1, \ldots, I$, and $k = 1, \ldots, K$.

Project II: Feature Selection for Different Samples

- ▶ Sample covariate x_i. Cord blood samples ($x_i = 0$). Healthy subject samples ($x_i = 1$).
- ▶ Binary indicator $\delta_{xk} \in \{0, 1\}$, $x = 0, 1$, and $k = 1, \ldots, K$, to indicate whether samples from x possess phenotype k
- ▶ $\delta_{xk} \mid p_x \overset{ind}{\sim}$ Bernoulli(p_x) and $p_x \overset{iid}{\sim}$ Beta(a_p, b_p).
- ▶ Unnormalized cell phenotype abundances
  $\tilde{w}_{ik} \overset{ind}{\sim}$ Gamma($a_W/K, 1$), $i = 1, \ldots, I$, and $k = 1, \ldots, K$.
- ▶ Relative abundances in sample i from x_i as
  $w_{ik} = \tilde{w}_{ik} \delta_{x_i k} / \sum_{\ell=1}^{K} \tilde{w}_{i\ell} \delta_{x_i \ell}$.
- ▶ Relative abundance w_{ik} is exactly zero for $\delta_{x_i k} = 0$.

Project II: Feature Selection for Different Samples

- Sample covariate x_i. Cord blood samples ($x_i = 0$). Healthy subject samples ($x_i = 1$).
- Binary indicator $\delta_{xk} \in \{0, 1\}$, $x = 0, 1$, and $k = 1, \ldots, K$, to indicate whether samples from x possess phenotype k
- $\delta_{xk} \mid p_x \overset{ind}{\sim} \text{Bernoulli}(p_x)$ and $p_x \overset{iid}{\sim} \text{Beta}(a_p, b_p)$.
- Unnormalized cell phenotype abundances
  $\tilde{w}_{ik} \overset{ind}{\sim} \text{Gamma}(a_W/K, 1)$, $i = 1, \ldots, I$, and $k = 1, \ldots, K$.
- Relative abundances in sample i from x_i as
  $w_{ik} = \tilde{w}_{ik} \delta_{x_i k} / \sum_{\ell=1}^{K} \tilde{w}_{i\ell} \delta_{x_i \ell}$.
- Relative abundance w_{ik} is exactly zero for $\delta_{x_i k} = 0$.
- Samples from x have the same subset of phenotypes but can have different relative abundances over the selected phenotypes.

Project II: Feature Selection for Different Samples

- ▶ Sample covariate x_i. Cord blood samples ($x_i = 0$). Healthy subject samples ($x_i = 1$).
- ▶ Binary indicator $\delta_{xk} \in \{0, 1\}$, $x = 0, 1$, and $k = 1, \ldots, K$, to indicate whether samples from x possess phenotype k
- ▶ $\delta_{xk} \mid p_x \stackrel{ind}{\sim} \text{Bernoulli}(p_x)$ and $p_x \stackrel{iid}{\sim} \text{Beta}(a_p, b_p)$.
- ▶ Unnormalized cell phenotype abundances $\tilde{w}_{ik} \stackrel{ind}{\sim} \text{Gamma}(a_W/K, 1)$, $i = 1, \ldots, I$, and $k = 1, \ldots, K$.
- ▶ Relative abundances in sample i from x_i as $w_{ik} = \tilde{w}_{ik}\delta_{x_i k} / \sum_{\ell=1}^{K} \tilde{w}_{i\ell}\delta_{x_i \ell}$.
- ▶ Relative abundance w_{ik} is exactly zero for $\delta_{x_i k} = 0$.
- ▶ Samples from x have the same subset of phenotypes but can have different relative abundances over the selected phenotypes.
- ▶ Phenotypes with $\delta_{0k} = \delta_{1k} = 1$ appear in all samples, while some are present in only one type of samples.

Project II: Feature Selection for Different Samples

- Sample covariate x_i. Cord blood samples ($x_i = 0$). Healthy subject samples ($x_i = 1$).
- Binary indicator $\delta_{xk} \in \{0, 1\}$, $x = 0, 1$, and $k = 1, \ldots, K$, to indicate whether samples from x possess phenotype k
- $\delta_{xk} \mid p_x \overset{ind}{\sim} \text{Bernoulli}(p_x)$ and $p_x \overset{iid}{\sim} \text{Beta}(a_p, b_p)$.
- Unnormalized cell phenotype abundances $\tilde{w}_{ik} \overset{ind}{\sim} \text{Gamma}(a_W/K, 1)$, $i = 1, \ldots, I$, and $k = 1, \ldots, K$.
- Relative abundances in sample i from x_i as $w_{ik} = \tilde{w}_{ik} \delta_{x_i k} / \sum_{\ell=1}^{K} \tilde{w}_{i\ell} \delta_{x_i \ell}$.
- Relative abundance w_{ik} is exactly zero for $\delta_{x_i k} = 0$.
- Samples from x have the same subset of phenotypes but can have different relative abundances over the selected phenotypes.
- Phenotypes with $\delta_{0k} = \delta_{1k} = 1$ appear in all samples, while some are present in only one type of samples.
- The probability models for the other parameters remain unchanged as in Project 1.

Project III: Feature Allocation Model with Regression for Feature Abundances Over Time

- $w_{t_1,k} = \xi_{t_1,k} / \sum_{\ell=1}^{K} \xi_{t_1,\ell}$

- We fix $\xi_{t_1,1} = a$, an arbitrary positive number, to avoid potential identifiability issues, and let $\xi_{t_1,k} = \max(\xi'_{t_1,k}, 0)$, for $k \geq 2$, where $\xi'_{t_1,k} \overset{iid}{\sim} \mathcal{N}(0, s_1^2)$

- $\xi_{t_i,k} = \max(\xi'_{t_i,k}, 0)$, $i = 2, \ldots, I$ and $k = 1, \ldots, K$

- $\xi'_{t_i,k} = \xi'_{t_1,k} + f_k(t_i)$, where $f_k(t_i)$ is a phenotype-specific function of time

- One choice is $f_k(t) = \xi'_{t_1,k} + \beta_{k1}t + \beta_{k2}t^2$